Nat Hazards
DOI 10.1007/s11069-012-0496-7

ORIGINAL PAPER

A study of earthquake inter-occurrence times distribution models in Taiwan

Chi-Hsuan Chen · Jui-Pin Wang · Yih-Min Wu · Chung-Han Chan · Chien-Hsin Chang

Received: 21 March 2012 / Accepted: 8 November 2012

Abstract Statistical studies on earthquake recurrence time probabilities have frequently been applied to seismic hazard analyses. In Taiwan, an instrumental catalog provides a good opportunity to examine statistical attributes of earthquakes around the study region, with the objective to evaluate the seismic risk and earthquake potential for hazard mitigation. With the completeness of recordings, seismic rates for small-to-moderate magnitudes can be obtained. An elimination of aftershocks was performed using a double-link cluster analysis method. The time intervals between a series of events (the inter-occurrence periods) are stationary with an identical temporal distribution. Based on the goodness-of-fit testing between a few models and observation, we suggested the use of the Gamma distribution in modeling this variable, earthquake inter-occurrence periods, for the study region. Accordingly, unified relationship was constructed, and statistical limitations of sparse sampling for devastating earthquakes (such as $M \geq 6.0$ or 7.0) could be resolved. The empirical result evaluated by introducing the conditional probability indicates that the recurrence probability of a $M \geq 7.0$ earthquake is 78.8 % within 10 years in Taiwan region.

Keywords Statistical seismology · Inter-occurrence periods · Gamma distribution · Recurrence probability

C.-H. Chen · Y.-M. Wu (✉) · C.-H. Chan
Department of Geosciences, National Taiwan University, No. 1, Sec. 4th, Roosevelt Rd., Taipei 10617, Taiwan
e-mail: drymwu@ntu.edu.tw

C.-H. Chen
Central Geological Survey, Ministry of Economic Affairs, New Taipei City 235, Taiwan

J.-P. Wang
Department of Civil and Environmental Engineering, The Hong Kong University of Science and Technology, Clear Water Bay, Kowloon, Hong Kong

C.-H. Chang
Central Weather Bureau, Taipei 100, Taiwan

Published online: 21 November 2012

1 Introduction

Taiwan is located within the plate boundary between the Philippine Sea Plate and the Eurasia Plate in an area generally threatened by damaging earthquakes. As a result of the combination of natural randomness and an inadequate knowledge of earthquake mechanisms, earthquake prediction seems difficult to achieve. However, statistical analyses provide another perspective for earthquake forecasts characterized by probability (Utsu 1972; Rikitake 1974; Hagiwara 1974). In the past few decades, studies and interests in earthquake forecasting have been increased. Many international cooperation projects have been proposed in order to establish platforms for scientific forecasting experiments, for example, the Collaboratory for the Study of Earthquake Predictability (CSEP; Jordan 2006); the Regional Earthquake Likelihood Models (RELM; Field 2007); The Seismic eArly warning For EuRope (SAFER; http://www.saferproject.net/); and the Network of Research Infrastructures for European Seismology (NERIES; http://www.neries-eu.org/). Through such integrated platforms, many scientists have proposed forecasting methods based on statistical experiences and/or physics-based models. Approaches include the following: Every Earthquake a Precursor According to Scale (EEPAS; Rhoades and Gerstenberger 2009); time–space Epidemic Type Aftershock model (ETAS; Kagan and Knopoff 1981, 1987; Ogata 1988); Proximity to Past Earthquake (PPE; Jackson and Kagan 1999); Short-term Aftershock Probability (STEP); and the rate-and-state friction model (Dieterich 1994). Also, several studies have been dedicated to modeling earthquake inter-occurrence times. Bak et al. (2002) found that two general power law distributions consisted of a separate time range that included individual events and aftershocks. Corral (2004, 2006) examined inter-occurrence periods of long-term earthquakes and proposed a universal scaling for temporal occurrence. Additionally, Saichev and Sornette (2006) proposed a simple theory for a universal scaling law, which is reached by a combination of some models as follows: the ETAS model treats all earthquakes on the same footing (no distinction between foreshocks, mainshocks, and aftershocks); the inter-occurrence time can be explained by Gutenberg–Richter distribution (Gutenberg and Richter 1944; Knopoff et al. 1982) and the Omori power laws (Utsu et al. 1995). The remarkable achievement of Saichev and Sornette (2006) is that the theory accounts quantitatively precisely for the empirical power laws found by Bak et al. (2002), Corral (2004, 2006), and the empirical statistics of inter-event times result from subtle crossovers rather than being genuine asymptotic scaling laws.

In order to obtain the rates of seismic occurrence, we predetermine the slope of frequency–magnitude distribution (FMD) of events, which is the b-value in the Gutenberg and Richter (G–R) relationship (Gutenberg and Richter 1944). The G–R relationship assumed that large earthquake samples the statistical distribution of small-to-moderate events, that is, frequency of large earthquake can be predicted from a distribution of small earthquake by extrapolating using a b-value. However, other studies (e.g., Utsu 1974; Purcaru 1975) pointed out that the observed numbers of events for large magnitude bins drop down sharply and deviate from a linear G–R relationship. Pacheco et al. (1992) checked the global seismicity catalog of shallow earthquakes from 1900 to 1989 and found a break in self-similarity by testing the b-value. The pronounced changes in the slope of FMD are observed at $M_s = 7.5$. For approaching the earthquake characteristics in Taiwan, we assumed a constant slope of FMD for local magnitude of $M \leq 7.0$, which were taken as following a constant b-value.

Talbi and Yamazaki (2009) provided an alternative Weibull distribution for modeling the timescales of moderate-to-large events in Southern California. Furthermore, a

transition model was proposed by Hasumi et al. (2009a, b, 2010) who tested some synthetic catalogs and three natural catalogs in Japan, Southern California, and Taiwan from 2001 to 2007. They suggested that the Weibull and log-Weibull combination model may best represent the universal distribution between different magnitudes for inter-occurrence period statistics of earthquakes. Although many inter-occurrence distribution models have been proposed, the universal feature in different regions is still open to debate. In this study, four temporal distribution reference models are tested in two stationary periods of time of these new selected catalogs, (i.e., the exponential, the Weibull, the Gamma, and the lognormal models). By comparing the fitness of models and empirical probabilities for the four models, we propose the best distribution model for the cumulative probability of inter-occurrence periods for Taiwan. We try to find a unique magnitude-independent relationship while rescale the inter-occurrence periods by the mean rates of seismic occurrence. Finally, we use the relationship of the frequency–magnitude distribution and forecast earthquake recurrence probability in different time windows after last events.

2 Data and methodology

2.1 Earthquake catalog

The earthquake catalog used in this study is originally collected by the Central Weather Bureau (CWB) and revised by Cheng et al. (2010). It provided more than 470,000 events from 1900 until 2010 with a focal depth of <40 km, which is the average crust thickness in Taiwan (Yeh and Tsai 1981; Lin 1996; Ustaszewski et al. 2012). We applied the method of spatiotemporal double-link cluster analysis to eliminate aftershocks in the catalog (Wu and Chiao 2006). This method is modified from the single-link cluster analysis proposed by Davis and Frohlich (1991). We supposed earthquakes with magnitude larger than magnitude threshold of 4.5 can be recognized as mainshocks. An event would be identified as an aftershock when its epicenter and occurrence time lay within the spatiotemporal window of mainshock. We set the temporal and spatial linking parameters of 3 days and 5 km and removed the aftershock events generated from mainshocks with $M \geq 4.5$. Those linking parameters are commonly used for earthquake declustering in Taiwan (Wu and Chiao 2006; Wu and Chen 2007; Wu et al. 2008a). Following the declustering process, a total of 364,308 earthquakes were used for the analysis (Fig. 1).

For accessing the distribution of parameters, the magnitude of completeness (M_c) for different catalogs needs to be examined in advance (Talbi and Yamazaki 2009). We evaluated using the maximum curvature method of Wiemer and Wyss (2000) through the software named "Zmap" (Wiemer 2001), shows M_c as a function of time (Fig. 2). Before 1973, a total of 15 stations equipped with Gray-Milne, Wiechert, and Omori seismographs (Hsu 1961) were maintained by the CWB. Before this time, M_c had a higher value of 4.3–4.8. After 1973, once the Taiwan Telemetric Seismic Network (TTSN) was established, M_c decreased to about $M_c = 2.0$–3.0. The TTSN consists of 25 stations within the Taiwan region. Real-time signals from field stations are transmitted to a central station via leased telephone lines (Wang 1989). Instruments in the old CWB seismic network have been gradually upgraded since 1981. In 1991, the TTSN was merged into the CWB seismic network and was upgraded to a real-time digital seismic network consisting of 75 stations (Wang and Shin 1998). The CWB seismic network has been changed since 1994 from a trigger recording mode to a continuous mode (Wu et al. 2008b). From then on, M_c values have significantly decreased to lower than 2.5.

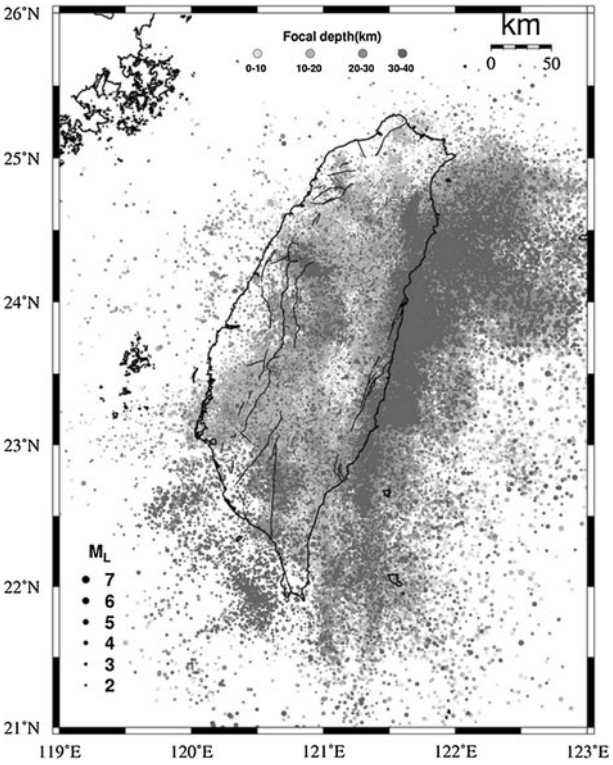

Fig. 1 The epicenter distribution of the declustered catalog surrounding Taiwan for a focal depth <40 km from 1900 to 2010

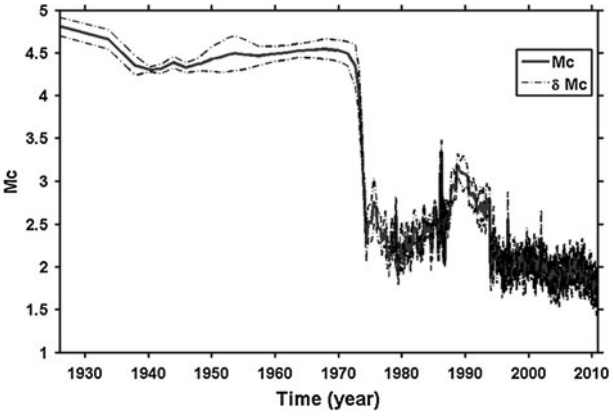

Fig. 2 Magnitude of completeness (M_c) as a function of time for the Taiwan region. *Dashed lines* show limits of bootstrap errors

Verifying whether or not a stationary process is inherited in seismicity catalog for an earthquake recurrence analysis is important (Corral 2006). Figure 3 shows cumulative earthquake occurrences as a function of time for both of clustered and declustered catalogs.

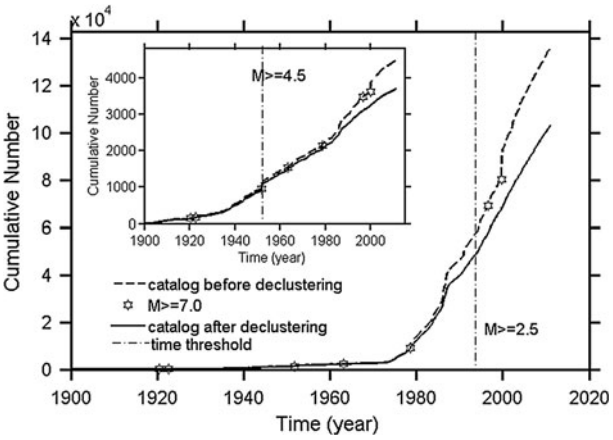

Fig. 3 The cumulative number of earthquakes before (*dash line*) and after (*solid line*) declustering from 1900 to 2010 for $M \geq 4.5$ and $M \geq 2.5$. The number of events for $M \geq 4.5$ and $M \geq 2.5$ are linear, increasing since 1952 and 1994, respectively. *Stars* show the occurrence of $M \geq 7.0$ events. *Dash-dot lines* show the time thresholds for the computation of the mean rate

After declustering, a lot of aftershocks occurred after large earthquakes were removed. For a stationary process, we considered the result of Figs. 2 and 3 to decide the time window for various magnitude thresholds. For $M \geq 4.5$, although there is an obvious lower down of M_c from 1940 to 1950 (Fig. 2), the time–frequency curve of the declustered catalog has a significant jump in 1951 (Fig. 3). This is due to some inland earthquakes with $M \geq 7.0$ occurred along the east coast of Taiwan. But the location quality is relatively poor in this area to discuss the relationship between mainshocks and aftershocks. For avoiding the fluctuating of seismicity rate, we chose the time period after 1952. For $M \geq 2.5$, once the TTSN was established after 1973, M_c decreased significantly (Fig. 2). But from the calculation of Fig. 2, the M_c value does not keep stable until 1990. For choosing the M_c satisfied with 2.5, we took the period during 1994 and 2010 into account, which corresponds to the network changed from a trigger recording mode to a continuous mode (Wu et al. 2008b). The minimum magnitude thresholds in the two periods can be considered as stationary.

Since the periods of stationary process were decided, we calculated the mean daily rate, R_w, of the catalog, which is defined as follows:

$$R_w = \frac{\text{cumulative earthquake numbers } (N)}{\text{time window (day)}}. \tag{1}$$

We evaluated R_w for different magnitudes using maximum likelihood estimation for liner regression function. Based on the earthquakes with $M_t = 2.5$–6.5 by steps of 0.5, the relationship between the daily seismic rate (R_w) and the magnitude threshold (M_t) can be expressed as follows:

$$\log R_w = 3.1791 - 0.908 M_t. \tag{2}$$

The linear trend with a constant slope in Fig. 4 is regarded as a magnitude-independent b-value. We are aware of some deviations from observed data with $M \geq 5.5$. This may be attributed to the limited amount of data because of short observation time. Based on this

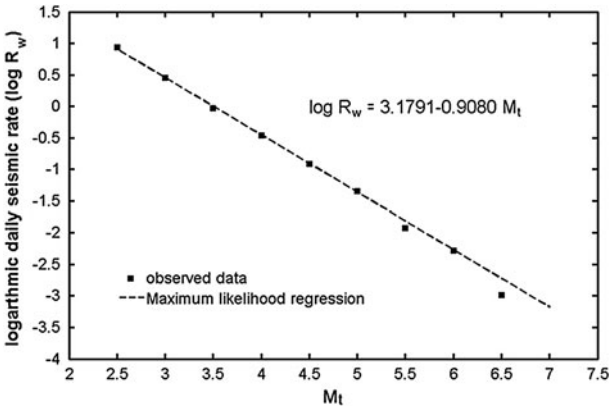

Fig. 4 The linear regression of observed data using maximum likelihood estimation between the daily seismic rate (R_w) and the magnitude threshold (M_t)

relationship, we obtained R_w of $M_t = 5.5$ to 1.53×10^{-2}/day, the R_w of $M_t = 6.0$ to 5.38×10^{-3}/day, and the R_w of $M_t = 7.0$ to 6.65×10^{-4}/day.

2.2 Inter-occurrence period

The inter-occurrence period (IOP) is defined as the time interval between consecutive events for a given M_t. Based on the definition, a series of IOPs could be obtained based on the catalog and the statistic parameters of IOPs in Table 1. We present the IOPs as a function of M_t in Fig. 5. The characteristics of the IOPs, such as time span and corresponding standard deviation, are presented. According to these parameters, the occurrence probability within a time elapse by using the theory of conditional probability can be calculated.

2.3 Statistical analysis and goodness-of-fit testing

As a practical consideration, we simply used four pure statistical distribution models for illustrating the distribution of earthquake recurrence periods in this study (i.e., the exponential, the Gamma, the lognormal, and the Weibull distributions/probability density function). The respective cumulative distribution functions $P_e(x)$, $P_g(x)$, $P_l(x)$, and $P_w(x)$ are expressed as follows:

$$p_e(x) = F(x;\delta) = 1 - \exp(-\delta x) \quad \text{for the exponential function;} \tag{3}$$

$$p_g(x) = F(x;\alpha,\beta) = \frac{\Gamma_{x/\beta}(\alpha)}{\Gamma(\alpha)} \quad \text{for the Gamma function;} \tag{4}$$

$$p_l(x) = F(x;\mu,\sigma) = \Phi\left(\frac{\ln x - \mu}{\sigma}\right) \quad \text{for the lognormal function;} \tag{5}$$

$$p_w(x) = F(x;\lambda,k) = 1 - e^{-\left(\frac{x}{\lambda}\right)^k} \quad \text{for the Weibull function,} \tag{6}$$

where $\delta, \alpha, \beta, \mu, \sigma, \lambda, k$ are the parameters of function $F(x)$ under the variable x, which is equal to each IOP in this article; Φ is the cumulative distribution function of the standard normal distribution; and Γ is the Gamma function.

Table 1 The statistic parameters of the IOPs with different M_t

Parameters	$M_t = 2.5$	$M_t = 3$	$M_t = 3.5$	$M_t = 4$	$M_t = 4.5$	$M_t = 5$	$M_t = 5.5$	$M_t = 6$
Mean (day)	0.117	0.354	1.068	2.946	8.401	23.144	89.209	276.419
Median (day)	0.070	0.209	0.645	1.836	4.496	12.973	50.714	165.602
Standard deviation (SD)	0.137	0.422	1.275	3.484	11.245	31.382	108.243	356.730
Time span (day)	1.832	4.462	14.515	28.597	121.538	424.343	657.794	1,819.904
Minimum (day)	0.000	0.000	0.000	0.000	0.000	0.000	0.003	0.073
Maximum (day)	1.832	4.462	14.515	28.597	121.538	424.343	657.797	1,819.977
Sum (day)	5,843.721	5,843.806	5,845.115	5,829.392	21,524.112	21,524.112	21,410.279	21,284.228
Number	50,102	16,510	5,472	1,979	2,562	930	240	77

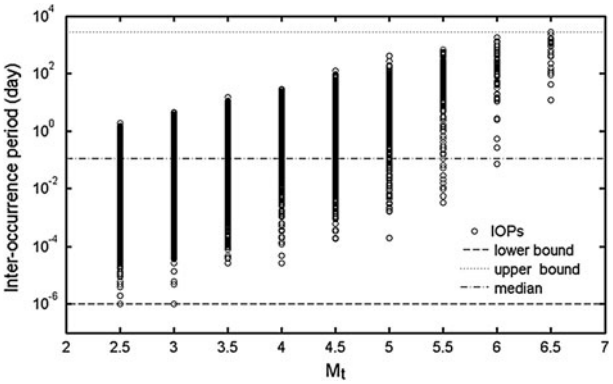

Fig. 5 The observed inter-occurrence periods (IOPs) as a function of magnitude thresholds (M_t). The *upper bound*, *lower bound,* and the *median* are included

In the following, we describe the root mean square (RMS), the Kolomogorov–Smirnov (*K–S*) test, the chi-square (χ^2) test, and Anderson–Darling test that were employed for testing the performance of each model.

The RMS can be expressed as follows:

$$\mathrm{RMS} = \sqrt{\frac{\sum_{i=1}^{N} [O_i - E_i]^2}{N}}, \tag{7}$$

where N is the sampling size; O_i is the observed cumulative probability; and E_i is expected cumulative probability at ith event with a given distribution model.

The Kolomogorov–Smirnov (*K–S*) test proposed by Chakravarti et al. (1967) is used to test the sample fitness with the specific distribution of continuous data. Based on the maximum difference (D_N) between these two curves, O_i and E_i, this test can be expressed as follows:

$$D_N = \max|O_i - E_i|. \tag{8}$$

The chi-square test is proposed by Snedecor and Cochran (1989). It can be applied to any univariant distribution for which we can calculate the cumulative distribution function. It is especially applied to classified data by comparing the observed frequencies and the expected frequencies computed with a given distribution model. As far as a continuous variable is concerned, a number of intervals are determined in advance for counting the respective frequency. We took the square root of event numbers as the number of bins (N) and calculate the following as the statistic of the chi-square (χ^2):

$$\chi^2 = \sum_{i=1}^{N} \frac{(O_i - E_i)^2}{E_i}, \quad E_i = N(F(B_\mathrm{u}) - F(B_\mathrm{L})), \tag{9}$$

where F is the specified cumulated distribution function; B_u and B_L are the upper and lower bounds for bin (i), respectively.

The Anderson–Darling test (A^2) (Stephens 1974) is a modification of the *K–S* test. This test has a higher weigh on tail data than the *K–S* test. The calculating of the A^2 test can be expressed as:

$$A^2 = -N - S \text{ and } S = \sum_{1}^{N} \frac{(2i-1)}{N} [\ln F(Y_i) + \ln(1 - F(Y_{N+1-i}))], \quad (10)$$

where Y_i are the ordered data from a distribution with cumulative distribution function, F.

According to the definitions of the four kind testings, a lower value of each test suggests a better fit between the observed and theoretical probabilities.

3 Results

3.1 The scaling of IOP

Goodness-of-fit testing was conducted in order to evaluate the appropriateness of the selected probability models for simulating IOP. Table 2 summarizes the parameters for the four models. It shows that the Gamma distribution generally has the best fit with the observed data, regardless of different M_t and testing methods.

According to the model parameters for different M_t's (Table 2), the cumulative Gamma distribution probabilities of the IOP were compared with observations (Fig. 6). For a fixed cumulative probability, the IOP becomes longer as M_t increases. Remarkably, different M_ts show similar shapes of cumulative density function for the $M_t = 2.5$–4.0 and $M_t = 4.5$–6.0, respectively. The shapes are a little different between the relative small and large dataset from visual inspection. Figure 6 also implies the impact of insufficient sampling on IOP observations for $M_t > 5.0$ that are not as smooth as those for small M_t's.

3.2 Rescale the IOP with the rate of seismic occurrence

The concept of the unified scaling law for the distribution of earthquake recurrence time (Corral 2004, 2006) was adopted in this study. In order to evaluate the applicability of the scaling law in Taiwan, $IOP \times R_w$ was used as the X-axis. The result indicates that the differences of IOPs between $M_t = 2.5$–4.0 mostly fell into a unified simple distribution (Fig. 7). It could be due to self-organized critical phenomena (Bak and Tang 1989). We checked the parameters of Gamma fitting of $M_t = 2.5$–4.0 in Table 2 and found the shape parameter, α, of Gamma distribution is at the range of 0.664 ± 0.032; the scale parameter, β, grows up with the time span. After rescaling, we put all the IOPs of $M_t = 2.5$–4.0 together and fit with the unique Gamma distribution model with $\alpha = 0.679$ and $\beta = 1.477$. Here, the unit of IOP is changed from day to year by dividing a value of 365.

After computing the unified IOP distribution up to $M_t = 4.0$, we rescaled the IOP data for $M_t = 4.5$ and tested their empirical distribution with that obtained by $M_t \leq 4.0$. We are aware of that the rescaled IOPs for $M_t = 4.5$ and 5.0 are slightly different with that of $M_t \leq 4.0$, which also can be found in different α-value in Table 2. As a result, another unified for $M_t \geq 4.5$ was constructed. A significant difference in α-value from $M_t \geq 5.5$ may be attributed to the insufficient data for the magnitude threshold.

Table 2 IOP statistical fittings for four distribution models comparing goodness of fit with the RMS, the K–S, the chi-squared, and the Anderson–Darling test

	Distribution	Parameters	RMS (rms)	K–S (Dn)	Chi-Squared (χ^2)	Anderson–Darling (A^2)
$M_t = 6$	IOP numbers = 77					
1	Exponential	$\delta = 266.999$	0.524	0.139	2.736	2.777
2	Gamma	$\alpha = 0.637$, $\beta = 434.125$	0.066	0.084	0.288	0.559
3	Lognormal	$\mu = 4.556$, $\sigma = 1.92$	0.214	0.135	3.430	2.258
4	Weibull	$\lambda = 233.567$, $k = 0.749$	0.018	0.106	0.089	1.014
$M_t = 5.5$	IOP numbers = 240					
1	Exponential	$\delta = 89.210$	0.682	0.119	17.699	10.695
2	Gamma	$\alpha = 0.558$, $\beta = 159.885$	0.240	0.057	15.074	1.726
3	Lognormal	$\mu = 3.372$, $\sigma = 2.243$	0.587	0.158	82.942	11.708
4	Weibull	$\lambda = 72.835$, $k = 0.694$	0.238	0.106	19.347	5.1,393
$M_t = 5$	IOP numbers = 930					
1	Exponential	$\delta = 23.144$	1.581	0.121	39.407	49.241
2	Gamma	$\alpha = 0.548$, $\beta = 42.218$	0.311	0.047	12.260	2.552
3	Lognormal	$\mu = 1.999$, $\sigma = 2.160$	1.153	0.139	222.551	34.153
4	Weibull	$\lambda = 18.390$, $k = 0.681$	0.398	0.071	25.265	9.755
$M_t = 4.5$	IOP numbers = 2,562					
1	Exponential	$\delta = 8.401$	3.011	0.138	320.201	173.95
2	Gamma	$\alpha = 0.530$, $\beta = 15.852$	0.337	0.026	22.711	3.969
3	Lognormal	$\mu = 0.941$, $\sigma = 2.149$	1.679	0.119	582.985	78.639
4	Weibull	$\lambda = 6.492$, $k = 0.661$	0.545	0.051	59.136	16.403
$M_t = 4$	IOP numbers = 1,979					
1	Exponential	$\delta = 2.946$	1.387	0.070	90.052	35.050
2	Gamma	$\alpha = 0.670$, $\beta = 4.40$	0.441	0.025	28.500	2.897
3	Lognormal	$\mu = 0.172$, $\sigma = 1.881$	1.535	0.118	460.819	67.702
4	Weibull	$\lambda = 2.596$, $k = 0.784$	0.472	0.061	34.812	19.260
$M_t = 3.5$	IOP numbers = 5,472					
1	Exponential	$\delta = 1.068$	2.554	0.081	348.792	135.640
2	Gamma	$\alpha = 0.642$, $\beta = 1.664$	0.768	0.028	53.558	9.967
3	Lognormal	$\mu = -0.888$, $\sigma = 1.913$	2.575	0.124	1,235.900	183.040
4	Weibull	$\lambda = 0.924$, $k = 0.761$	0.837	0.054	88.432	43.644
$M_t = 3$	IOP numbers = 16,510					
1	Exponential	$\delta = 0.354$	4.897	0.087	1,854.900	454.930
2	Gamma	$\alpha = 0.648$, $\beta = 0.546$	0.772	0.025	115.737	21.249
3	Lognormal	$\mu = -1.981$, $\sigma = 1.829$	4.049	0.105	3,067.700	428.480
4	Weibull	$\lambda = 0.306$, $k = 0.763$	1.044	0.035	250.932	59.752
$M_t = 2.5$	IOP numbers = 50,102					
1	Exponential	$\delta = 0.117$	7.720	0.078	4,994.300	1,012.300
2	Gamma	$\alpha = 0.696$, $\beta = 0.168$	0.581	0.017	190.395	23.911
3	Lognormal	$\mu = -3.018$, $\sigma = 1.693$	6.400	0.094	7,627.900	1,026.700
4	Weibull	$\lambda = 0.103$, $k = 0.797$	1.153	0.023	526.900	73.270

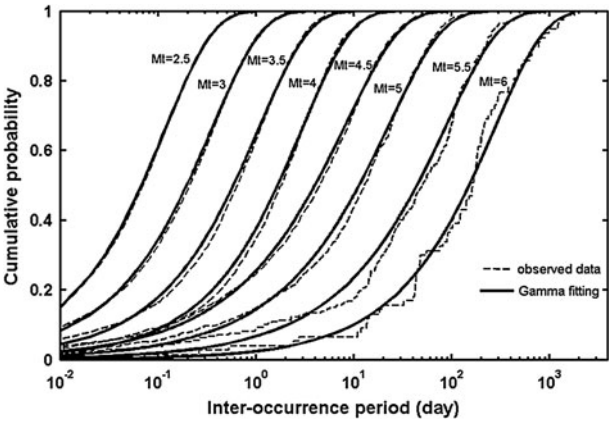

Fig. 6 The observed (*dashed lines*) cumulative probabilities of the inter-occurrence periods (IOPs) and the corresponding Gamma model fitting (*solid lines*) using magnitude thresholds (M_t) from 2.5 to 6.0

4 Discussion

4.1 The temporal distribution of large earthquakes

Universal scaling law studies (Corral 2004, 2006) have determined IOP distribution functions that are close to a generalized Gamma distribution. Based on Corral's studies, the scaling law is the relationship between the average probability densities, and we may derive discrete probability due to the time period that grows as logarithmic binning. For this study, we replaced the discrete function with a cumulative probability function and derived observations by statistical fitting.

Based on the definition of the Gamma distribution in Eq. (4), "α" is the parameter that controls the shape of distribution, whereas "β" is the scaled parameter. According to the modeled cumulative probabilities as a function of $IOP \times R_w$ through the Gamma distribution, the changes in the shape parameters of IOP probabilities are insensitive to magnitude (small variations of α-values). However, we discriminated pronounced different IOP probabilities for the two magnitude ranges ($M_t = 2.5$–4.0 and $M_t \geq 4.5$) (Fig. 7). The discrete behaviors for the two magnitude ranges correspond to the discovery by Hasumi et al. (2010). Thus, we assumed respective fixed shape (constant α-value) for each magnitude range. For evaluating α-value of the larger magnitudes ($M_t \geq 4.5$), we only took the events with $M_t = 4.5$–5.0 for avoiding the influence of insufficient recording. We obtained the α-value of 0.537 for the magnitude range. Based on this result, $\beta = 0.987$ and 7.988 are further acquired for $M_t = 6.0$ and 7.0, respectively. The scaling relationship makes it possible to identify for the distribution of larger magnitudes even without sufficient records.

4.2 Fitting with the Weibull distribution

By comparing the goodness-of-fit testing (Table 2), the Gamma distribution generally fits the observed data best. But in two cases ($M_t = 5.5$ and 6.0), the performance of RMS in the Weibull distribution is better than the Gamma model. To understand the fitting differences between the two models, we applied the IOP of $M_t \geq 4.5$ for testing. Figure 8 indicates that the two distributions are very close to the observed data and both may be

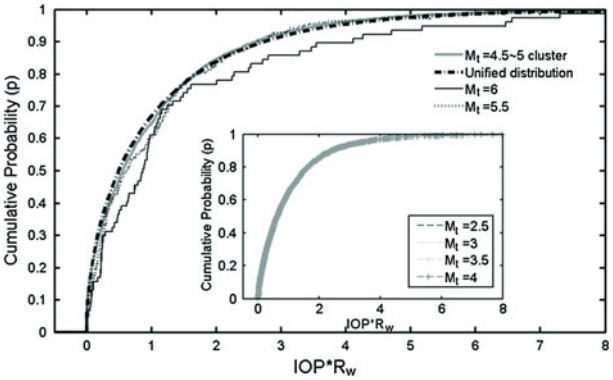

Fig. 7 The collapsed distributions of rescaled data for two magnitude ranges $M_t = 2.5$–4.0 and $M_t = 4.5$–5.0, respectively, fitted with a unified Gamma model. The distributions of $M_t \geq 5.5$ departed from those of $4.5 \leq M_t \leq 5.0$. This result can be attributed to the data insufficient. R_w's are all from the observational results

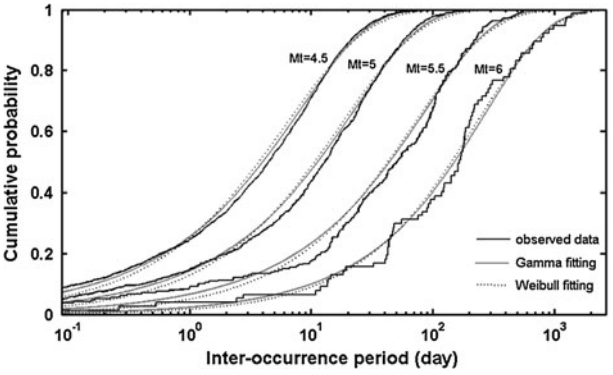

Fig. 8 Comparison between observation, Gamma, and Weibull models. The two models are very close to the observations. The Weibull distribution forecasts a lower probability in the shortest and longest part of IOP and higher in the middle part of IOP relate to the Gamma distribution and observed data

capable for portraying the scale relationship between the cumulative probability and IOPs. It is noteworthy that the Weibull distribution tends to underestimate the probability in the shortest and longest part of IOP and overestimates in the middle part of IOP relate to the Gamma distribution and observed data. It suggests that the Gamma distribution is more consistent with the observed data.

4.3 The recurrence probabilities of large earthquakes

Previous studies (Savage 1992; Schwartz and Coppersmith 1984; Shimazaki and Nakata 1980; Jacob 1984) used the conditional probability as a forecast indicator of the stress reconstruction in a single seismogenic structure. In this study, by contrast, we applied the earthquake prognosis on the statistics of recurrence time in a region, which covers several seismogenic structures. Corral (2006) considered both worldwide and southern California seismic catalogs, in which the distribution of the recurrence times strongly depend on the

Table 3 The rescale parameters (α, β) calculated using the unified IOP Gamma distribution and the probabilities in future years

M_t	α	β	Te (years)	Occurrence probability (%) in future (Tp)		
				1 year	10 years	20 years
6.0	0.537	0.987	1.155	70.4	99.9	100
6.1	0.537	1.217	6.208	58.6	99.9	100
6.2	0.537	1.500	6.208	51.6	99.9	99.9
6.3	0.537	1.849	6.208	45.0	99.7	99.9
6.4	0.537	2.279	6.208	39.0	99.1	99.9
6.5	0.537	2.808	6.208	33.6	98.0	99.9
6.6	0.537	3.461	6.208	28.8	96.1	99.8
6.7	0.537	4.266	6.208	24.7	93.2	99.5
6.8	0.537	5.258	6.208	21.1	89.2	98.7
6.9	0.537	6.481	6.208	18.0	84.4	97.2
7.0	0.537	7.988	6.208	15.4	78.8	94.9

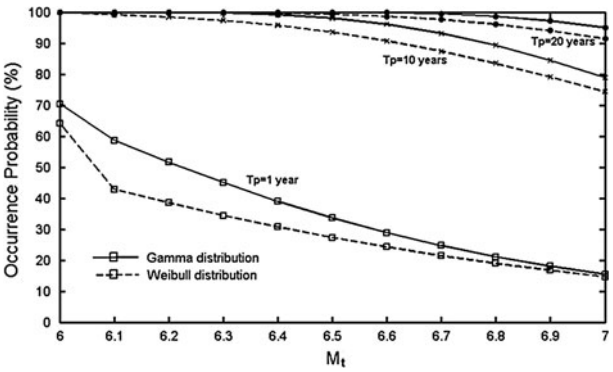

Fig. 9 Recurrence probabilities derived from the Gamma and Weibull distributions for earthquake magnitude thresholds (M_t) from 6.0 to 7.0 in the future 1, 10, and 20 years

previous recurrence time. It could imply that it can be applied either for a local area or a large region, which covers several seismogenic structures. As a consequence, the occurrence probability within a time elapse after last event requires an adjustment using the theory of conditional probability. The probability for the next occurrence between the shortest (Te) and longest period (Tp) time can be expressed as the Gamma distribution $P_g(Tp|Te)$:

$$P_g(Tp|Te) = \frac{P_g(Te + Tp) - P_g(Te)}{1 - P_g(Te)}, \tag{11}$$

where P_g is the cumulative probability following a Gamma distribution.

For a specific magnitude of exceedance, parameters of the distribution models were rescaled from $IOP \times R_w$ to IOP. Table 3 shows rescale parameters for the unified Gamma distribution and calculated probabilities given different periods of time, respectively. To compare with the probabilities derived from the Weibull model (dashed line in Fig. 9), the

Gamma model presents slightly higher occurrence probability of next event within 1 and 20 year(s). The recurrence probabilities (Gamma model) for an earthquake with a $M \geq 7.0$ are 15.4, 78.8, and 94.9 %, for 1, 10, and 20 year(s), respectively. The result shows good agreement with a study that estimated the recurrence probability of large earthquakes based on annual maximum earthquake magnitudes since 1900 (Wang et al. 2011). For example, within 10 years, in comparison with the 78.8 % obtained in this study, the probability obtained by Wang et al. (2011) for a $M \geq 7.0$ earthquake was about 85 % for the region surrounding Taiwan.

5 Conclusions

The study provides a reliable and effective procedure in determining the optimal model for simulating the time interval between a series of earthquakes. In our analysis, we discriminate different behaviors of the IOP probability for the two magnitude ranges and the Gamma model fit best among them. According to Hasumi et al. (2010), the discrete behaviors for two magnitude ranges could be interpreted as the plate-driven damaging mechanics changes. The unified relationship of rescaled IOPs used to determine the fitting parameters may reduce the impact of insufficient sampling of large earthquakes. According to the empirical result evaluated by introducing the conditional probability, the recurrence probability of a $M \geq 7.0$ earthquake is 15.4 and 94.9 % within 1 and 20 year(s) in Taiwan region, respectively.

Acknowledgments We thank Paul Wessel and Walter Smith for developing and supporting the GMT mapping tools. This work was supported by Central Geological Survey, Central Weather Bureau, and the National Science Council, Taiwan. We thank Prof. Thomas Glade and two anonymous reviewers for their constructive comments.

References

Bak P, Tang C (1989) Earthquakes as a self-organized critical phenomenon. J Geophys Res 94(B11): 15635–15637

Bak P, Christensen K, Danon L, Scanlon T (2002) Unified scaling law for earthquakes. Phys Rev Lett 88(178501):1–4

Chakravarti IM, Laha RG, Roy J (1967) Handbook of methods of applied statistics, vol 1. Wiley, Volume I, pp 392–394

Cheng SN, Wang TB, Lin TW, Jiang CH (2010) Establishment of Taiwan earthquake catalog, vol 54. Seismology Technical Report of Central Weather Bureau, pp 575–605

Corral Á (2004) Long-term clustering, scaling, and universality in the temporal occurrence of earthquakes. Phys Rev Lett 92:108501

Corral Á (2006) Dependence of earthquake recurrence times and independence of magnitudes on seismicity history. Tectonophys 424:177–193

Davis SD, Frohlich C (1991) Single-link cluster analysis of earthquake aftershocks: decay laws and regional variations. J Geophys Res 96:6336–6350

Dieterich JH (1994) A constitutive law for rate of earthquake production and its application to earthquake clustering. J Geophys Res 99(B2):2601–2618

Field EH (2007) Overview of the working group for the development of regional earthquake likelihood models (RELM). Seismol Res Lett 78(1):7–16

Gutenberg B, Richter CF (1944) Frequency of earthquakes in California. Bull Seismol Soc Am 34:185–188

Hagiwara Y (1974) Probability of earthquake occurrence as obtained from Weibull distribution analysis of crustal strain. Tectonophys 23:313–318

Hasumi T, Akimoto T, Aizawa Y (2009a) The Weibull-log Weibull transition of the interoccurrence time statistics in the two-dimensional Burridge-Knopoff Earthquake model. Phys A 388:483–490

Hasumi T, Akimoto T, Aizawa Y (2009b) The Weibull-log Weibull distribution for interoccurrence times of earthquakes. Phys A 388:491–498
Hasumi T, Chen CC, Akimoto T, Aizawa Y (2010) The Weibull-log Weibull transition of interoccurrence time for synthetic and natural earthquakes. Tectonophys 485:9–16
Hsu MT (1961) Seismicity in Taiwan (Formosa). Bull Earthq Res Int Tokyo Univ 29:831–847
Jackson DD, Kagan YY (1999) Testable earthquake forecasts for 1999. Seismol Res Lett 70(4):393–403
Jacob KH (1984) Estimates of long-term probabilities for future great earthquakes in the Aleutians. Geophys Res Lett 11:295–298
Jordan TH (2006) Earthquake predictability, brick by brick. Seismol Res Lett 77(1):3–6
Kagan YY, Knopoff L (1981) Stochastic synthesis of earthquake catalogs. J Geophys Res 86:2853–2862
Kagan YY, Knopoff L (1987) Statistical short-term earthquake prediction. Science 236(4808):1563–1567
Knopoff L, Kagan Y, Knopoff R (1982) b-values for fore- and aftershocks in real and simulated earthquake sequences. Bull Seismol Soc Am 72:1663–1676
Lin CH (1996) Crustal structures estimated from arrival differences of the first P-waves in Taiwan. J Geol Soc China 39:1–12
Ogata Y (1988) Statistical models for earthquake occurrence and residual analysis for point processes. J Am Stat As 83:9–27
Pacheco JF, Scholz CH, Sykes LR (1992) Changes in frequency-size relationship from small to large earthquakes. Nature 355:71–73
Purcaru G (1975) A new magnitude-frequency relation for earthquakes and a classification of relation types. Geophys J R Astron Soc 42:61–79
Rhoades DA, Gerstenberger MC (2009) Mixture models for improved short-term earthquake forecasting. Bull Seismol Soc Am 99(2):636–646
Rikitake T (1974) Probability of an earthquake occurrence as estimated from crustal strain. Tectonophys 23:299–312
Saichev A, Sornette D (2006) Universal distribution of inter-earthquake times explained. Phys Rev Lett 97:078501
Savage JC (1992) The uncertainty in earthquake conditional probabilities. Geophys Res Lett 19:709–712
Schwartz DP, Coppersmith KJ (1984) Fault behavior and characteristic earthquakes-examples from the Wasatch and San Andreas fault zones. J Geophys Res 89:5681–5698
Shimazaki K, Nakata T (1980) Time-predictable recurrence model for large earthquakes. Geophys Res Lett 7:279–282
Snedecor GW, Cochran WG (1989) Statistical methods, 8th edn. Iowa State University Press, Iowa
Stephens MA (1974) EDF statistics for goodness of fit and some comparisons. J Am Stat As 69:730–737
Talbi A, Yamazaki F (2009) Sensitivity analysis of the parameters of earthquake recurrence time power law scaling. J Seismol 13(1):53–72
Ustaszewski K, Wu YM, Suppe J, Huang HH, Chang CH, Carena S (2012) Crust-mantle boundaries in the Taiwan–Luzon arc-continent collision system determined from local earthquake tomography and 1D models: Implications for the mode of subduction polarity reversal. Tectonophysics. doi:10.1016/j.tecto.2011.12.029 (in press)
Utsu T (1972) Large earthquakes near Hokkaido and the expectancy of the occurrence of a large earthquake of Nemuro. Rep Coord Comm Earthq Predict 7:7–13
Utsu T (1974) A three-parameter formula for magnitude distribution of earthquake. J Phys Earth 22:71–85
Utsu T, Ogata Y, Matsuura S (1995) The centenary of the Omori formula for a decay law of aftershock activity. J Phys Earth 43:1–33
Wang JH (1989) The Taiwan telemetered seismographic network. Phys Earth Planet Inter 58:9–18
Wang CY, Shin TC (1998) Illustrating 100 years of Taiwan Seismicity. Terr Atmos Ocean Sci 9:589–614
Wang JP, Chan CH, Wu YM (2011) The distribution of annual maximum earthquake magnitude around Taiwan and its application in the estimation of catastrophic earthquake recurrence probability. Nat Hazard. doi:10.1007/s11069-011-9776-x
Wiemer S (2001) A software package to analyse seismicity: ZMAP. Seismol Res Lett 72:373–382
Wiemer S, Wyss M (2000) Minimum magnitude of completeness in earthquake catalogs: examples from Alaska, the Western United States, and Japan. Bull Seismol Soc Am 90(4):859–869
Wu YM, Chen CC (2007) Seismic reversal pattern for the 1999 Chi–Chi, Taiwan, Mw7.6 earthquake. Tectonophys 429:125–132
Wu YM, Chiao LY (2006) Seismic quiescence before the 1999 Chi–Chi, Taiwan Mw7.6 earthquake. Bull Seismol Soc Am 96:321–327
Wu YM, Chen CC, Zhao L, Chang CH (2008a) Seismicity characteristics before the 2003 Chengkung, Taiwan, earthquake. Tectonophys 457:177–182

Wu YM, Chang CH, Zhao L, Teng TL, Nakamura M (2008b) A comprehensive relocation of earthquakes in Taiwan from 1991 to 2005. Bull Seismol Soc Am 98:1471–1481
Yeh YH, Tsai YB (1981) Crustal structures of central Taiwan from inversion of P-wave arrival times. Bull Inst Earth Sci 1:83–102